

Available online at [www.sciencedirect.com](http://www.sciencedirect.com)**ScienceDirect**

Procedia Engineering 126 (2015) 372 – 376

**Procedia  
Engineering**[www.elsevier.com/locate/procedia](http://www.elsevier.com/locate/procedia)

7th International Conference on Fluid Mechanics, ICFM7

# Direct numerical simulation of three-dimensional gravity current on a uniform slope

A. Ooi<sup>a,\*</sup>, N. Zgheib<sup>b</sup>, S. Balachandar<sup>b</sup><sup>a</sup>*Department of Mechanical Engineering, The University of Melbourne, Parkville 3010, Australia*<sup>b</sup>*Department of Mechanical and Aerospace Engineering, University of Florida, USA*

---

## Abstract

Gravity currents occur when fluids of different density are brought together. When gravity currents travel down a uniform slope, buoyancy effects become more important and changes the physical dynamics of its motion. In the present paper, we report data from full three-dimensional direct numerical simulation of gravity currents propagating down a uniform slope. Our data shows that in most cases, the gravity current evolve to a shape that is similar to a triangular wedge. The physical mechanisms leading to formation of this triangular shape and the dynamics of such a structure is presented

© 2015 Published by Elsevier Ltd. This is an open access article under the CC BY-NC-ND license (<http://creativecommons.org/licenses/by-nc-nd/4.0/>).

Peer-review under responsibility of The Chinese Society of Theoretical and Applied Mechanics (CSTAM)

**Keywords:** gravity currents; direct numerical simulations; boussinesq

---

## 1. Introduction

Gravity are relevant in many engineering applications such as the dispersion of hazardous gas cloud or the spillage heavy chemicals from marine vehicles. Gravity currents are also the chief mechanism responsible for backdraft, when oxygen is suddenly introduced to a fire trapped in an enclosure and is a real threat to firefighters ([1]). Another example of gravity current are powder-snow avalanches where the entrainment of heavier fine grained snow maintains a density difference between the avalanche and ambient air enabling the powder-snow avalanche to reach velocities as high as 100m/s ([2]).

---

\* Corresponding author. Tel.: +61 3 8344 6732; fax: +61 3 9347 8784.  
E-mail address: [asho@unimelb.edu.au](mailto:asho@unimelb.edu.au)

**Nomenclature**

$\bar{h}$	equivalent height
$p$	non-dimensional pressure
$\rho$	non-dimensional density
$u$	non-dimensional velocity field
$u_F$	velocity of front of gravity current
$V_0^*$	dimensional initial volume
$x_F$	position of front of gravity current

Laboratory experiments ([3,4]) and numerical simulations ([5,6,7]) of finite release gravity currents in canonical setups (axisymmetric and planar releases on horizontal boundaries) reveal that in general, a gravity current transitions through four main stages. A single, short lived, initial acceleration phase at the end of which the current attains its maximum velocity. A slumping phase succeeds the acceleration phase, it is characterized with a roughly uniform front height and a front speed that is constant or nearly constant. Following the slumping phase, the current transitions into the self-similar inertial phase where the front velocity decreases as a power law ([8]). Finally, viscous forces become important and a second self-similar regime is observed, termed the viscous phase. Here again the current's front velocity decays as a power law, however at a faster rate than in the inertial phase ([8]).

For gravity currents travelling down a slope, most of the studies thus far have concentrated on “planar” release ([7,9]) currents. Experimental study of such a current ([9]) showed that its properties are predominantly two-dimensional and its statistics are homogeneous in the spanwise direction. Entrainment effects are significant and the head of the gravity current increases in size as it travels down the slope. With the advent of supercomputers, researchers can now conduct high fidelity simulations of “planar” current traveling down a slope. Using DNS data, [10] assessed the validity of using thermal theory to predict the properties of the gravity current head.

For a “circular” release travelling down a uniform slope, the dynamics of the gravity current is quite different to a “planar” current. The current shape is altered as buoyancy and the sloping surface break the axisymmetry and makes the large-scale flow fully three-dimensional. Such flow consideration has many practical relevance such as powder-snow avalanches and turbidity currents driven by mud slides. Even so, studies of three-dimensional currents propagating down a uniform slope are relatively scarce. Theoretical investigations have been conducted by [11] who predicted that the gravity current will assume a self-similar circular wedge shape. [12] expanded on the study by [11] to include the effects of entrainment. [13] carried out experiments and showed that contrary to the prediction of [11], the gravity current takes on a shape that is more akin to a triangular wedge.

In the present manuscript, we report data from fully-resolved three-dimensional direct numerical simulation (DNS) of Boussinesq gravity currents propagating down a uniform slope starting from a truncated cylinder initial shape.

## 2. Direct numerical simulation

### 2.1. Numerical model

The configuration of the simulation is designed to mimic the experimental study of [13]. We model the release a finite amount of heavy fluid into an ambient environment of lighter fluid on a sloping boundary. We assume the density difference is small and use the Boussinesq approximation. The non-dimensional system of equations governing the evolution of the flow can be written as

$$\nabla \cdot \mathbf{u} = 0, \quad (1)$$

$$\frac{D\mathbf{u}}{dt} = \rho \mathbf{e}^g - \nabla p + \frac{1}{\text{Re}} \nabla^2 \mathbf{u}, \quad (2)$$

$$\frac{\partial \rho}{\partial t} + \nabla \cdot (\rho \mathbf{u}) = \frac{1}{\text{Sc Re}} \nabla^2 \rho. \quad (3)$$

Here,  $\mathbf{u}$ ,  $\rho$ ,  $p$ , represent the divergence free non-dimensional velocity field, density, and pressure respectively. The non-dimensional density  $\rho$  is defined as

$$\rho = \frac{\rho^* - \rho_a^*}{\rho_{c0}^* - \rho_a^*}. \quad (4)$$

The asterisk denotes a dimensional quantity and the variables  $\rho^*$ ,  $\rho_a^*$ , and  $\rho_{c0}^*$  represent the local, ambient, and initial heavy fluid densities, respectively. Therefore, the value of  $\rho$  remains bounded between 0 and 1. The dimensionless pressure is given by

$$p = \frac{p^*}{\rho_a^* (U^*)^2}, \quad (5)$$

where  $p^*$  and  $U^*$  denote the local dimensional pressure and velocity scale, respectively.  $\mathbf{e}^g$  is a unit vector pointing in the direction of gravity and the Schmidt,  $\text{Sc}$ , and Reynolds number,  $\text{Re}$ , are defined as

$$\text{Sc} = \frac{\nu^*}{\kappa^*}, \quad \text{Re} = \frac{\Lambda^* U^*}{\nu^*}, \quad (6)$$

where  $\nu^*$  and  $\kappa^*$  represent the kinematic viscosity and molecular diffusivity of the current. We follow [13] and define the length scale  $\Lambda^*$ , the velocity scale  $U^*$ , and the time scale  $T^*$  as

$$\Lambda^* = (V_0^*)^{1/3}, \quad U^* = \sqrt{g^* \frac{\rho_{c0}^* - \rho_a^*}{\rho_a^*} \Lambda^*}, \quad T^* = \frac{\Lambda^*}{U^*}, \quad (7)$$

where  $V_0^*$  is the initial volume of heavy fluid in the truncated cylinder, and  $g^*$  denotes the gravitational acceleration.

Equations (1) – (3) are solved using a spectral code ([8]). In the wall normal,  $z$ -direction, no slip boundary condition is used for the velocity field at the bottom wall and a free slip boundary condition is used at the top wall. Periodic boundary conditions are used for all variables in the streamwise,  $x$ , and spanwise,  $y$ , directions. This implies that a periodic array of gravity currents is being simulated. Hence, care must be taken to ensure that these currents do not interact as we are interested in the development of an isolated gravity current. The length of the domain in the spanwise direction is chosen to ascertain that there is uninterrupted development of the gravity current. As for the density field, zero gradient conditions are enforced at the top and bottom boundaries.

Trial and error have shown that using a domain size of  $L_x=18$  and  $L_y=15$  is sufficient to ensure that there is no side “contamination” from the spanwise periodic boundary conditions. Simulations were carried out at  $\text{Re}=5000$  and a grid resolution of  $(N_x, N_y, N_z)=(700, 600, 201)$  and slope angle  $\theta=5^\circ, 10^\circ, 15^\circ$ , and  $20^\circ$ . The value of the Schmidt number is taken as unity for all simulations. In the experiments of [13], the Schmidt number is much greater than 1. However, [14] have shown that the Schmidt number only has a small effect on the dynamics and structure of the gravity current, provided the Reynolds number is high enough ( $O(10^4)$ ). For smaller Reynolds number, diffusion effects will influence the mixing and front velocity of the gravity current. The time step is chosen such that the Courant number is always less than 0.5.

### 3. Results

#### 3.1. Spatial structure and mass distribution

In order to aid with the presentation of results, we will define the equivalent height,

$$\bar{h} = \int \rho dz$$

which is the integrated height of the current in the wall normal,  $z$ , direction.  $\bar{h}$  gives an indication of the distribution of mass in the streamwise and spanwise directions and is a good representation of the shape of the gravity current. The evolution of  $\bar{h}$  for  $\theta = 15^\circ$  shown in Fig. 1. Low values of  $\bar{h}$  is shown in blue and high values of  $\bar{h}$  is coloured red. The maximum value of  $\bar{h}$  and the corresponding time value are shown in the figure. At  $t=1$ , most of the mass is concentrated at the centre of the current. At a later point in time,  $t=2$ , the mass moves towards the circumference of the current. As the current propagates down the slope, the mass moves along the circumference of the current towards the front. As a result, the gravity current forms a triangular wedge shape with most of mass concentrated at the current front. This triangular shape (at  $t=6$  and  $t=10$  in Fig. 1) agrees very well with the experimental observations of [13].

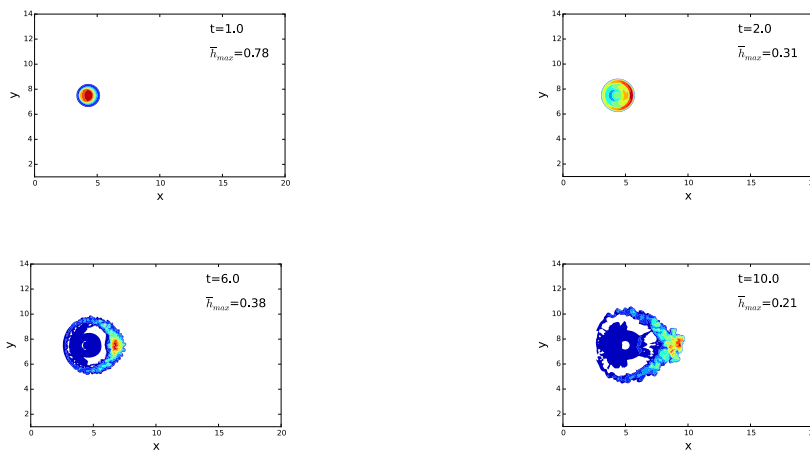


Fig. 1. Evolution of  $\bar{h}$  at  $Re=5000$  and  $\theta = 15^\circ$

#### 3.2. Front location and velocity

To investigate how fast the current moves down the slope, the position of the current front,  $x_F(t)$ , for  $\theta = 15^\circ$  is plotted as a function of time in Fig. 2 (left). The front position is taken as the maximum streamwise location of a small threshold value  $\epsilon=10^{-2}$  of the current  $\bar{h}$ . We observe very good agreement between our simulations (solid line) and the published experimental data (symbols). Similar agreement is observed for all values of  $\theta$ .

The front velocity is obtained by differentiating the front location with respect to time using a central (3 point stencil) finite difference scheme. Figure 2(right) shows the temporal evolution of the front velocity  $u_F(t)$  for the four slopes. The small circles represent the front velocity of the simulations as obtained from a central finite difference scheme. The solid line is there to illustrate the trend and is obtained by running a numerical filter through the raw data. The velocity curves reveal some very interesting dynamics that have not been reported before. Unlike circular release gravity currents that spread on horizontal flat surfaces, the downhill slope makes gravitational effects more important and gives rise to a second acceleration phase immediately following the first acceleration phase. With the exception of the  $\theta=20^\circ$  case, the maximum velocity achieved by the gravity current is at the end of

the first acceleration phase. At the end of the first acceleration phase, the current redistributes itself and undergoes a second acceleration phase to propel the front velocity to a local maximum value. The presence of the second acceleration phase indicates a rearrangement or redistribution of the heavy material within the current to increase the buoyancy at the downstream end of the current near the centerline ( $y=0$  plane). The second acceleration is not found in studies of “planar” (or two-dimensional) gravity currents, or cylindrical, axisymmetric currents on horizontal boundaries.

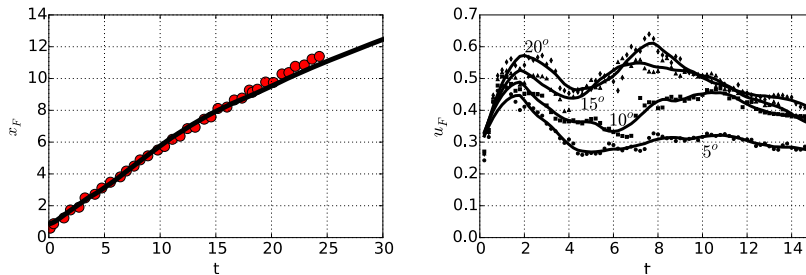


Fig. 2. Location of current front  $Re = 5000$  and  $\theta = 15^\circ$  (left) and velocity of current for  $\theta=5^\circ, 10^\circ, 15^\circ$ , and  $20^\circ$  (right).

#### 4. Conclusions

We present data from highly resolved numerical simulations to investigate the dynamics of a circular finite release on a sloping boundary. Simulations were carried out at  $Re = 5000$  with four different slopes ( $\theta=5^\circ, 10^\circ, 15^\circ$ , and  $20^\circ$ ). The shape of the release was chosen to conform to previous experiments of [13]. The simulations predict that the current evolve to a triangular wedge shape which agrees with experimental observations. The predicted current's front position also compares very well with the experimental data. Calculations of the current front velocity reveal that the gravity current transition through two acceleration phases. This is a new result and we attribute it to the rearrangement or redistribution of the heavy material “focusing” the mass towards the front of the current.

#### References

- [1] Fleischmann, C. M., & McGrattan, K. B. 1999. Numerical and experimental gravity currents related to backdrafts. *Fire Safety Journal* **33**, 21–34.
- [2] Turnbull, B., & McElwaine, J. N. 2007. A comparison of powder-snow avalanches at Vallee de la Sionne, Switzerland, with plume theories. *Journal of Glaciology* **53**, 30–40.
- [3] Huppert, H. E. & Simpson, J. 1980. The slumping of gravity currents. *J. Fluid Mech.* **99**, 785–799.
- [4] Marino, B. M., Thomas, L. P., & Linden, P. F. 2005. The front condition for gravity currents. *J. Fluid Mech.* **536**, 49–78.
- [5] Cantero, M., Lee, J. R., Balachandar, S. & Garcia, M. 2007a. On the front velocity of gravity currents. *J. Fluid Mech.* **586**, 1–39.
- [6] Blanchette, F., Strauss, M., Meiburg, E., Kneller, B., Glinisky, M. 2005. High-resolution numerical simulations of resuspending gravity currents: condition for self-sustainment. *J. Geophys. Res.* **110**, c12022.
- [7] Dai, A. 2013. Experiments on gravity currents propagating on different bottom slopes. *J. Fluid Mech.* **731**, 117–141.
- [8] Cantero, M. I., Balachandar, S. & Garcia, M. H. 2007b. High-resolution simulations of cylindrical density currents. *J. Fluid Mech.* **590**, 437–469.
- [9] Britter, R. E. & Linden, P. F. 1980. The motion of the front of a gravity current travelling down an incline. *J. Fluid Mech.* **99**, 531–543.
- [10] Dai, A., Ozdemir, C. E., Cantero, M. I., & Balachandar, S. 2012. Gravity Currents from Instantaneous Sources Down a Slope. *J. Hydraulic Eng.* **138**, 237–246.
- [11] Webber, D. M., Jones, S. J., & Martin, D. 1993. A model of the motion of a heavy gas cloud released on a uniform slope. *J. Hazard. Mater.* **33**, 101–122.
- [12] Tickle, G. A. 1996. A model of the motion and dilution of a heavy gas cloud released on a uniform slope in calm conditions. *J. Hazard. Mater.* **49**, 29–47.
- [13] Ross, A. N., Linden, P. F., & Dalziel, S. B. 2002. A study of three-dimensional gravity currents on a uniform slope. *J. Fluid Mech.* **453**, 239–261.
- [14] Bonometti T. & Balachandar S. 2008 Effect of Schmidt number on the structure and propagation of density currents. *Theor. Comput. Fluid Dyn.* **22**, 341–361.